The electrochemical performance of super P carbon black in reversible Li/Na ion uptake

Peng, Bo; Xu, Yaolin; Wang, Xiaoqun; Shi, Xinghua; Mulder, Fokko M.

DOI
10.1007/s11433-017-9022-y

Publication date
2017

Document Version
Accepted author manuscript

Published in
Science China: Physics, Mechanics and Astronomy

Citation (APA)
Peng, B., Xu, Y., Wang, X., Shi, X., & Mulder, F. M. (2017). The electrochemical performance of super P carbon black in reversible Li/Na ion uptake. *Science China: Physics, Mechanics and Astronomy*, *60*(6), 1-8. Article 064611. https://doi.org/10.1007/s11433-017-9022-y

SCIENCE CHINA
Physics, Mechanics & Astronomy

• Article •

January 2016 Vol.59 No.1: 000000
doi: 10.1007/s11433-000-0000-0

The electrochemical performance of super P carbon black in reversible Li/Na ion uptake

Bo Peng [1,2††], Yaolin Xu[2††], Xiaoqun Wang[1,3], Xinghua Shi[4] and Fokko M. Mulder[2,*]

[1] *Department of Physics, Renmin University of China, No. 59 Zhongguancun Street, Haidian District, Beijing, 100872, China*
[2] *Materials for Energy Conversion and Storage (MECS), Department of Chemical Engineering, Faculty of Applied Science, Delft University of Technology, Van der Maasweg 9, 2629 HZ Delft, The Netherlands*
[3] *Department of Physics and Astronomy, Shanghai Jiao Tong University, No. 800 Dongchuan Road, Minhang District, Shanghai, 200240,China*
[4] *National Center for Nanoscience and Technology (NCNST), No.11 Zhongguancun Beiyitiao, Beijing, 100190, China*

Received January 1, 2016; accepted January 1, 2016; published online January 1, 2016

Super P carbon black (SPCB) has been widely used as a conducting additive in Li/Na ion batteries to improve the electronic conductivity. However, there has not yet been a comprehensive study on its structure and electrochemical properties for Li/Na ion uptake, though it is important to characterize its contribution in any study of active materials that uses this additive in non-negligible amounts. In this article the structure of SPCB has been characterized and a comprehensive study on the electrochemical Li/Na ion uptake capability and reaction mechanisms are reported. SPCB exhibits a considerable lithiation capacity (up to 310 mAh g^{-1}) from the Li ion intercalation in the graphite structure. Sodiation in SPCB undergoes two stages: Na ion intercalation into the layers between the graphene sheets and the Na plating in the pores between the nano-graphitic domains, and a sodiation capacity up to 145 mAh g^{-1} has been achieved. Moreover, the influence of the type and content of binders on the lithiation and sodiation properties has been investigated. The cycling stability is much enhanced with sodium carboxymethyl cellulose (NaCMC) binder in the electrode and fluoroethylene carbonate (FEC) in the electrolyte; and a higher content of binder improves the Coulombic efficiency during dis-/charge.

Super P carbon black, Li ion batteries, Na ion batteries

PACS number(s): 81.05.U-, 82.45.Yz, 82.47.Aa, 82.47.Cb

Citation: A. Author, B. Author, and C. Author, *Sample manuscript for SCPMA*, Sci. China-Phys. Mech. Astron. **59**, 000000 (2016), doi: 10.1007/s11433-000-0000-0

1 Introduction

Nowadays Li ion batteries play a dominant role in the rechargeable battery market and Na ion batteries have received increasing research attention due to the growing demand of cost-effective and high energy density energy storage devices and the much higher abundance of sodium compared to lithium. Significant progress has been made in recent years [1-6].

Carbonaceous materials have been extensively studied as the anode candidates for Li/Na ion batteries because of the excellent electrochemical stability and cost-effectiveness [7-10]. Graphite (372 mAh g^{-1} for LiC_6) has been commercially applied as the anode for Li ion batteries exhibiting a low working voltage and a high specific capacity. However, graphite turns out to be not suitable for Na ion storage [11, 12]. This difference results from the different reaction mechanisms between lithiation and sodiation in graphitic

---

*Corresponding author (email: F.M.Mulder@tudelft.nl)
††These authors contributed equally to this work.

carbon. Li ions are intercalated in the graphite structure forming graphite intercalation compounds (GICs) [13]. However, it is not thermodynamically favorable to form Na ion based GICs [14], though it can occur in expanded graphite [15], and solvated Na ion intercalation can take place in graphite [16, 17]. Hard carbon (disordered carbon, low graphitization level) appears to be most suitable for Na ion uptake [5, 9]. The sodiation mechanism in hard carbon has been mostly interpreted with a "card-house" model including two stages [18]: (1) Na ion intercalation between the graphene sheets during the sloping voltage range; (2) Na plating in the pores between nano-graphitic domains during the voltage plateau near 0 V.

Super P carbon black (SPCB), which is produced from partial oxidation of petrochemical precursors, exhibits a large specific surface area and superb electrical conductivity, and because of these properties has been widely used as a conducting additive in the electrodes to improve the electronic conductivity in Li/Na ion batteries [19]. However, despite that there are some minor referral electrochemical measurements on SPCB, there has not been a comprehensive study on the electrochemical properties of SPCB itself, and very limited knowledge on the structure and reaction mechanisms for Li/Na ion uptake has been reported. Since the SPCB can be added in non-negligible amounts in various applications, its Li/Na insertion characteristics are important to characterize. Especially since carbon is also an active material for reversible Li/Na ion storage, the capacity and working potential range of SPCB for Li/Na ion uptake must be determined to figure out the electrochemical performance of the active materials *excl.* SPCB in the electrodes.

Moreover, the electrochemical performance of SPCB working with different binding materials and electrolytes in Li/Na ion batteries has not been investigated yet. Even if binders make up only a minor portion of the electrode, it may in some cases play a critical role in the electrochemical activities of the Li/Na ion batteries [20, 21]. Polyvinylidene fluoride (PVDF) is the mainstream binder in commercial batteries and research, but it is not suitable for the high-capacity alloy-based electrode materials (e.g. Si and Sn) exhibiting significant volume changes; Instead, water soluble binders, such as sodium carboxymethyl cellulose (NaCMC) and polyacrylic acid (PAA), etc. attract intensive attention in these high capacity alloy-based electrode materials (e.g. Si) because of their higher adhesivity and elasticity compared with PVDF, as well as their lower cost, easier processing and environmental benignity. Furthermore, the addition of fluoroethylene carbonate (FEC) and / or vinylene carbonate (VC) has been frequently employed for the alloy-based electrodes to form a more compact solid electrolyte interface (SEI) layer and thus to achieve a stable cycling performance [22-24].

This article presents a comprehensive study on the electrochemical Li/Na ion uptake performance of SPCB. The morphology and structure of SPCB have been characterized; its capability and electrochemical performance for Li/Na ion storage have been studied and the lithiation and sodiation mechanisms have been elucidated. Furthermore, the influences of PVDF and NaCMC binders and their contents in the electrode on the electrochemical Li/Na ion uptake properties have been investigated.

2 Experimental Details

Electrode fabrication: The electrode was fabricated with a conventional slurry based method. Specifically, commercial SPCB (TIMCAL) was mixed with a binder with different mass ratios of SPCB, 90 % and 60 %, respectively, in a solvent. Two types of binder, PVDF and NaCMC, were investigated, and N-Methyl-2-pyrrolidone (NMP) and deionized water, respectively, were used as the solvent correspondingly. The mixing was assisted with magnetic stirring until a homogeneous slurry was obtained. Then the slurry was cast onto a Cu foil (12.5 μm, Goodfellow) with a doctor blade. After initial drying at room temperature overnight, the electrode was transferred into a vacuum working at 70 ℃ for 12 hours. Finally, the electrode was mechanically compacted with a roller compressor and cut into circular pieces for battery assembly. The mass loading of active materials on the electrodes amounted to ~ 1.0 mg cm^{-2}.

Battery assembly: Half-cell Li / Na ion batteries were assembled in an argon atmosphere glovebox (O_2 / H_2O: < 0.1 ppm) using Li/Na foil as the counter electrode and Borosilicate glass microfiber as the separator. The electrolyte varied depending on the battery types and binders as below:

Li ion half-cells: For the PVDF binder based electrodes, 1.0 mol/L $LiPF_6$ in ethylene carbonate (EC) and dimethyl carbonate (DMC) (EC : DMC = 1 : 1 in volume) was used as the working electrolyte. For the NaCMC based electrodes, the working electrolyte was 1.0 mol/L $LiPF_6$ in EC/DMC = 1 : 1 with 10 % FEC.

Na ion half-cells: For the PVDF binder based electrodes, 1.0 mol/L $NaClO_4$ dissolved in EC and propylene carbonate (PC) (EC : PC = 1 : 1 in volume) was used as the working elecctrolyte; For the NaCMC based electrodes, the working electrolyte was 1.0 mol/L $NaClO_4$ in EC/PC = 1 : 1 with 10 % FEC.

Electrochemical measurement: Galvanostatic electrochemical performance of the Super P carbon black based Li/Na half-cells were tested between 0.01 V and 2.0 V with a Maccor 4600 battery cycler. Cyclic voltammetry (CV) was performed with a PGSTAT302N Autolab potentiostat with a cut-off voltage of 0.005 V and 2.0 V for discharge and charge, respectively.

Characterization: Scanning Electron Microscope (SEM) images were taken with a JEOL JSM 6010F scanning electron microscope operating at an accelerating voltage of 10 kV. X-ray Diffraction (XRD) was performed with a Cu K_α source PANalytical X'Pert Pro PW3040/60 diffractometer working at 45 kV and 40 mA. The Raman spectrum of SPCB was obtained with a Thermo Scientific Nicolet Almega XR Dispersive Raman Spectrometer.

3 Results and Discussions

3.1 Characterization on SPCB

The SEM images (**Figure 1a-1c**) show that SPCB appears to be extremely porous, flocculent, cross-linked carbon nanothreads. **Figure 1d** shows that it is poorly crystalline as no distinct X-ray diffraction peaks can be observed, revealing its disordered nature in lattice parameter ranges. Two extremely broad peaks are observed at $2\theta = 25.3°$ and $42.8°$, which correspond to the Bragg reflection on the lattice planes (002) and (100) of carbon. The characteristic D (1360 cm^{-1}) and G band (1580 cm^{-1}) of carbon are evidenced in the Raman shift of SPCB (**Figure 1e**). The G band originates from the graphitic structure of SPCB, and the D band indicates the structural defects / disorder. The significant D band peak together with the amorphous XRD pattern of SPCB reveals its substantial structural disorder and low graphitization level.

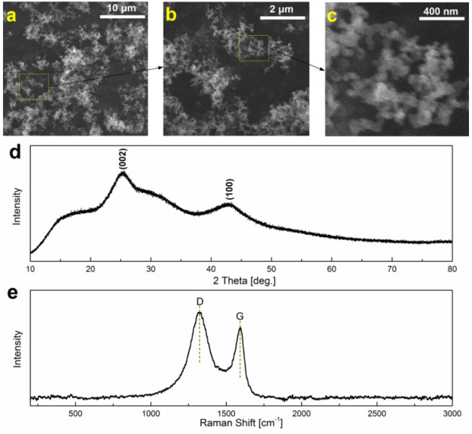

Figure 1 Characterization on SPCB. (a) - (c), SEM images at different magnifications; (d), XRD pattern; (e) Raman spectrum.

3.2 SPCB based Li ion batteries

Galvanostatic electrochemical lithiation performance of the SPCB based electrodes has been characterized by testing it within Li ion half-cells. **Figure 2a** shows that with cycling at C/3 (C = 300 mA g^{-1}) the 60 % SPCB - PVDF electrode achieves an initial reversible capacity of 213 mAh g^{-1} for Li ion storage, which is relatively lower compared to the 90 % SPCB - PVDF electrode that achieves a delithiation capacity of 230 mAh g^{-1} for the first cycle. However, the cycling stability of the 60 % SPCB - PVDF electrode appears to be superior compared to the other. Specifically, the capacity retention of the 60 % SPCB - PVDF electrode reaches 203 mAh g^{-1} in 70 cycles, which is 95.3 % of the initial reversible capacity. In comparison, after 70 cycles the 90 % SPCB - PVDF electrode retains only 90.8 % of its initial delithiation capacity. This may be explained by the relatively higher Coulombic Efficiency (**Figure A1** in Appendix) of the 60 % SPCB - PVDF electrode because more binder enables stronger elasticity and mechanical strength of the electrode and thus the structural integrity has been maintained along cycling.

Figure 2b demonstrates that initial reversible Li insertion capacities of 229 mAh g^{-1} and 231 mAh g^{-1} can be achieved for 90 % and 60 % SPCB - NaCMC electrodes, respective, which is comparable with the PVDF based electrodes. However, the capacity retentions of the NaCMC based electrodes increase slightly and both reach 247 mAh g^{-1} after 70 cycles, which is different from the gradually deteriorating PVDF based electrodes. This can be probably attributed to not only the superior adhesive quality and elasticity of NaCMC but the formation of a more compact SEI layer upon the presence of FEC as described in the introduction.

Both the PVDF and NaCMC based SPCB electrodes exhibit an excellent rate capability in Li ion batteries when the current rate varies between C/15 and 2C. However, the electrodes using NaCMC, compared to PVDF, appear to show improved reversible capacity for Li ion storage, which may indicate its superior binding capability and/or the formation of a more stable SEI layer (**Figure 2c-2d**). For the PVDF based electrodes, the capacity reaches ~ 250 mAh g^{-1} at C/15, and ~ 160 mAh g^{-1} can be achieved when the cycling rate increases to 2C. In comparison, the NaCMC based electrodes achieves > 280 mAh g^{-1} and ~195 mAh g^{-1} at C/15 and 2C, respectively, and the electrode containing 60% active materials even achieves a capacity of up to 310 mAh g^{-1} for Li ion storage.

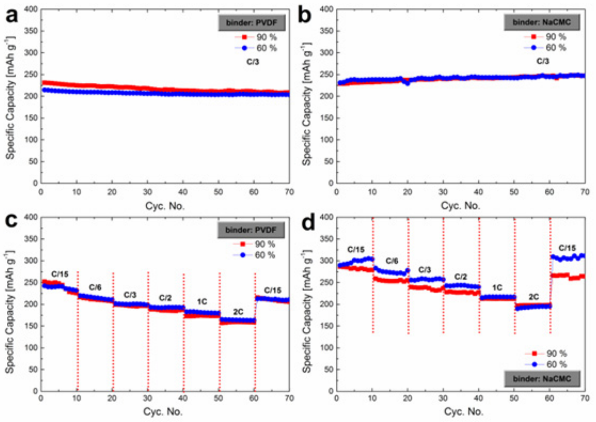

Figure 2 Electrochemical Li ion storage performance of the SPCB based electrodes containing 90% and 60% of active materials: reversible capacity retentions of the SPCB electrodes with (a), PVDF and (b), NaCMC binder cycling at C/3, and the rate capabilities of the electrodes that use (c), PVDF and (d), NaCMC as the binder. (C = 300 mA g^{-1})

3.3 SPCB based Na ion batteries

The electrochemical (de-)sodiation performance of the SPCB based electrodes has been measured by cycling the electrodes within Na ion half-cells.

Figure 3a reports that the 60 % SPCB - PVDF electrode obtains an initial desodiation capacity of 131 mAh g^{-1} cycling at C/3, which degrades gradually during the first few cycles and then becomes stable. The retained capacity reaches 119 mAh g^{-1}, 90.5 % of the initial capacity; the 90 % SPCB - PVDF electrode achieves a reversible capacity of 122 mAh g^{-1} for the first cycle and 88.5 % of that can still be retained after 70 cycles. This can also be interpreted with the improved Coulombic efficiency when more binder is present (**Figure A2** in Appendix). In comparison, as is demonstrated in **Figure 3b**, the 60 % and 90 % SPCB - NaCMC based electrodes reach a reversible capacity ~ 110 mAh g^{-1} for Na ion storage and keep stable along cycling, no apparent degradation has been observed which indicates the relatively superior binding capability of NaCMC for SPCB.

Figure 3c-3d shows that the rate capability of the electrode for Na ion batteries follows a similar capacity decreasing trend when the current rate increases as what has been observed in Li ion batteries. Reversible capacities of ~ 145 mAh g^{-1} and ~ 75 mAh g^{-1} can be achieved at C/15 and 2C, respectively, for the PVDF based SPCB electrodes. The 90 % SPCB - NaCMC electrode achieves capacities of 126 mAh g^{-1} and 70 mAh g^{-1}, respectively, at C/15 and 2C. The 60 % SPCB - NaCMC electrode has a desodiation capacity of 128 mAh g^{-1} in the first cycle and it grows gradually and reaches 135 mAh g^{-1} after 10 cycles; 79 mAh g-1 can be still achieved when the battery is dis-/charged at 2C. When the cycling rate is reset at C/15, a capacity of 135 mAh g^{-1} is restored, indicating its excellent rate capability.

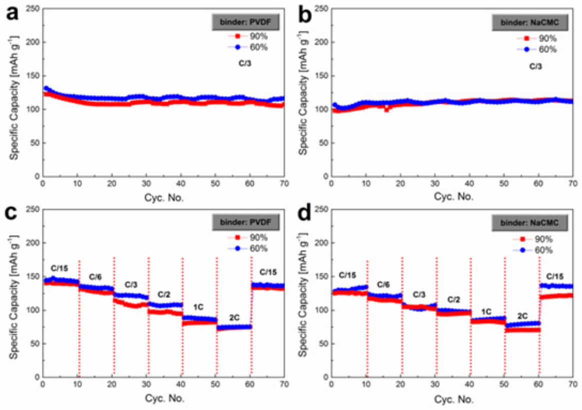

Figure 3 Electrochemical Na ion storage performance of the SPCB based electrodes containing 90% and 60% of active materials: reversible capacity retentions of the SPCB electrodes that use (a), PVDF and (b), NaCMC binder cycling at C/3, and the rate capabilities of the electrodes using (c), PVDF and (d), NaCMC as the binder. (C = 300 mA g^{-1})

3.4 Discussion

Comparing the electrochemical performance of SPCB for Na ion batteries with that for Li ion batteries, the reversible capacity of SPCB for Na ion storage is relatively lower compared with that for Li ion, which will be related to the different mechanisms between lithiation and sodiation. The lithiation results from Li ion intercalation in graphite structures of SPCB. In contrast, due to the low graphitization level of SPCB as observed in **Figure 1**, Na ion uptake in SPCB probably follows the "card-house" model in which two stages would be present: Na ion intercalation in the layers between the graphene sheets and Na nano-plating in the pores between the nano-graphitic domains in SPCB.

Moreover, the electrodes with a larger amount of binders exhibit a better cycling stability in both Li and Na ion batteries, thanks to the better structural integrity upon the presence of higher content of binding materials. However, different from what has been observed in the performance of the SPCB based Li ion batteries, the reversible sodiation capacities of NaCMC based electrodes are relatively lower than that of the PVDF based electrodes. Following the "card-house" model for Na uptake in pores this may possibly originate from a lower accessibility of the pores between nano-graphitic domains in SPCB. This should then be a result of the presence of a different more strongly adhesive and elastic NaCMC.

The major irreversible capacity loss for the SPCB based Li/Na ion batteries originates from the irreversible SEI formation, which mostly takes place in the first Li/Na ion uptake cycle. Specifically, a voltage plateau at ~ 0.8 V is observed in the initial lithiation voltage profile of the SPCB - PVDF electrode, which disappears after the first cycle (**Figure 4a**), associated with the irreversible SEI formation. Similar phenomenon is also evidenced in the galvanostatic voltage profile of the SPCB - PVDF electrode for Na ion battery (**Figure 4b**). The plateau for SEI formation during initial sodiation appears at a different voltage (~ 0.6 V) from the lithiation process. (The voltage profiles of the SPCB - NaCMC electrodes for Li/Na ion batteries are demonstrated in **Figure A3a-A3b** in Appendix.)

This SEI formation is also evidenced in the cyclic voltammetry (CV) measurements (**Figure 4c-4d**). A cathodic peak is observed at 0.6 V and 0.4 V for initial lithiation and sodiation, respectively, which is not visible in the following cycles corresponding to the irreversible SEI formation. These voltages are lower than the voltages that have been observed in the galvanostatic voltage profiles, resulting from the higher overpotentials.

The overpotential is dominated by the internal resistance of the battery and the current rate for dis-/charge. The galvanostatic voltage profiles of Li/Na ion batteries (**Figure 4a-4b** & **A3a-A3b**) appear to be quite symmetric indicating a low overpotential between charge and discharge process. This can be attributed to the low resistance because of the electrical conducting nature of SPCB. The overpotential may increase along cycling as the local stress in the electrode increases and the resistance grows [25]. When the cycling rate increases the overpotentials grow and thus leads to the earlier voltage cut-off and the capacity drop as observed in the rate capability tests (**Figure 2c-2d** & **3c-3d**).

Furthermore, the de-/lithiation of SPCB mainly takes place at a low voltage range, and a sloping voltage < 1.2 V is observed in the galvanostatic voltage profiles (**Figure 4a** & **A3a**) attributed to the Li ion intercalation in the graphite structure. The de-/sodiation occurs at an even lower voltage range (< 0.8 V), and the voltage profiles can be divided into two stages, one sloped decreasing voltage range > 0.1 V and the other voltage plateau ~ 0.05 V (**Figure 4b** & **A3b**). This can be explained with the two reaction stages ("card-house" model) during sodiation and is also consistent with the cyclic voltammograms (**Figure 4c-4d**).

The consequence of the sloping voltage profiles will be that in a low potential Li/Na ion anode (e.g. Li-Si or Na-P) the SPCB will largely be lithiated or sodiated at a higher potential than where the main lithiation or sodiation of the active materials take place. For higher potential anodes (such as $Li_4Ti_5O_{12}$) or cathodes no lithiation or sodiation of SPCB will take place.

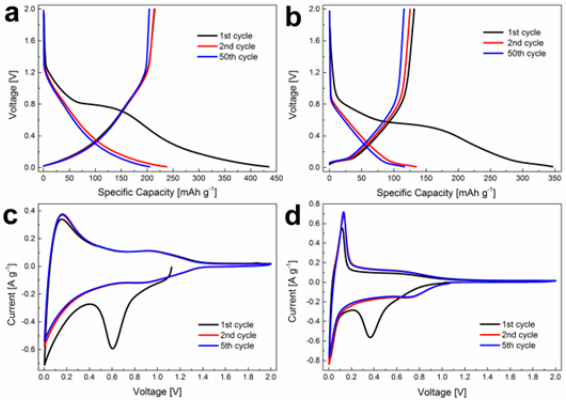

Figure 4 Voltage profile of the SPCB based (a), Li and (b), Na ion anode at 1st, 2nd and 50th cycle cycling at C/3; and cyclic voltammograms of the SPCB based (c), Li and (d), Na ion anode at 1st, 2nd and 5th cycle. (scan rate: 0.5 mV s^{-1}) Here the Li/Na ion battery anodes contain 60% SPCB and 40% PVDF.

4 Conclusions

In this article, the structure of SPCB has been studied and its performance for the reversible electrochemical Li and Na ion storage has been investigated by testing it within Li/Na half-cells. SPCB exhibits a high reversible lithiation capacity, up to 310 mAh g^{-1}, which mainly originates from the Li ion intercalation in the graphite structure of SPCB. The reversible sodiation capacity reaches up to 145 mAh g^{-1} and it undergoes the "card-house" mechanism. Moreover, SPCB shows excellent rate capability for both Li and Na ion uptake; and the cycling stability is much enhanced upon the presence of NaCMC binder and FEC addition in the electrolyte. Additionally, a higher content of binder in the SPCB electrode improves the Coulombic efficiency during dis-/charge, which is indicative of a higher resilience against contact losses due to structural alterations.

In summary, despite the different reaction mechanisms, SPCB exhibits a considerable capability of electrochemical Li/Na ion uptake and the performance varies in different environments. The electrochemical Li/Na ion uptake properties of SPCB reported in this article will provide a reference for the research on Li/Na ion battery electrodes that utilize significant amounts of SPCB as a conductive additive.

This work is financially supported by the Chinese Scholarship Council (CSC), Opening fund of State Key Laboratory of Nonlinear Mechanics and the 'A green Deal in Energy Materials' (ADEM) grant funded by Dutch Ministry of Economic Affairs and ADEM industrial partners.

[1] M. Armand, J.M. Tarascon, Nature, 451 (2008) 652-657.
[2] Y. Sun, N. Liu, Y. Cui, Nat. Energy, (2016) 16071.
[3] G. E. Blomgren, J. Electrochem. Soc. **164**, A5019 (2017).
[4] B. L. Ellis, and L. F. Nazar, Curr. Opin. Solid State Mater. Sci. **16**, 168 (2012).
[5] H. Kim, H. Kim, Z. Ding, M. H. Lee, K. Lim, G. Yoon, and K. Kang, Adv. Energ. Mater. **6**, 1600943 (2016).
[6] K. Kubota, and S. Komaba, J. Electrochem. Soc. **162**, A2538 (2015).
[7] Y. Liu, Y. M. Wang, B. I. Yakobson, and B. C. Wood, Phys. Rev. Lett. **113**, 028304 (2014), arXiv: 1401.6671.
[8] F. Yao, D. T. Pham, and Y. H. Lee, ChemSusChem **8**, 2284 (2015).
[9] W. Luo, F. Shen, C. Bommier, H. Zhu, X. Ji, and L. Hu, Acc. Chem. Res. **49**, 231 (2016).
[10] E. Irisarri, A. Ponrouch, and M. R. Palacin, J. Electrochem. Soc. **162**, A2476 (2015).
[11] P. Ge, and M. Fouletier, Solid State Ion. **28**, 1172 (1988).
[12] A. Metrot, D. Guerard, D. Billaud, and A. Herold, Synth. Met. **1**, 363 (1980).
[13] J. R. Dahn, T. Zheng, Y. Liu, and J. S. Xue, Science **270**, 590 (1995).
[14] K. Nobuhara, H. Nakayama, M. Nose, S. Nakanishi, and H. Iba, J. Power Sources **243**, 585 (2013).
[15] Y. Wen, K. He, Y. Zhu, F. Han, Y. Xu, I. Matsuda, Y. Ishii, J. Cumings, and C. Wang, Nat. Commun. **5**, 4033 (2014).
[16] B. Jache, and P. Adelhelm, Angew. Chem. Int. Ed. **53**, 10169 (2014).
[17] H. Kim, J. Hong, Y. U. Park, J. Kim, I. Hwang, and K. Kang, Adv. Funct. Mater. **25**, 534 (2015).
[18] D. A. Stevens, and J. R. Dahn, J. Electrochem. Soc. **147**, 1271 (2000).
[19] Q. Zhang, Z. Yu, P. Du, and C. Su, Recent Pat. Nanotech. **4**, 100 (2010).
[20] S. L. Chou, Y. Pan, J. Z. Wang, H. K. Liu, and S. X. Dou, Phys. Chem. Chem. Phys. **16**, 20347 (2014).
[21] W. Zhang, M. Dahbi, and S. Komaba, Curr. Opin. Chem. Eng. **13**, 36 (2016).
[22] M. Nie, J. Demeaux, B. T. Young, D. R. Heskett, Y. Chen, A. Bose, J. C. Woicik, and B. L. Lucht, J. Electrochem. Soc. **162**, A7008 (2015).
[23] L. Ji, M. Gu, Y. Shao, X. Li, M. H. Engelhard, B. W. Arey, W. Wang, Z. Nie, J. Xiao, C. Wang, J. G. Zhang, and J. Liu, Adv. Mater. **26**, 2901 (2014).
[24] K. Schroder, J. Alvarado, T. A. Yersak, J. Li, N. Dudney, L. J. Webb, Y. S. Meng, and K. J. Stevenson, Chem. Mater. **27**, 5531 (2015).
[25] F. Q. Yang, Sci. China-Phys. Mech. Astron. **59**, 114611 (2016).

Appendix

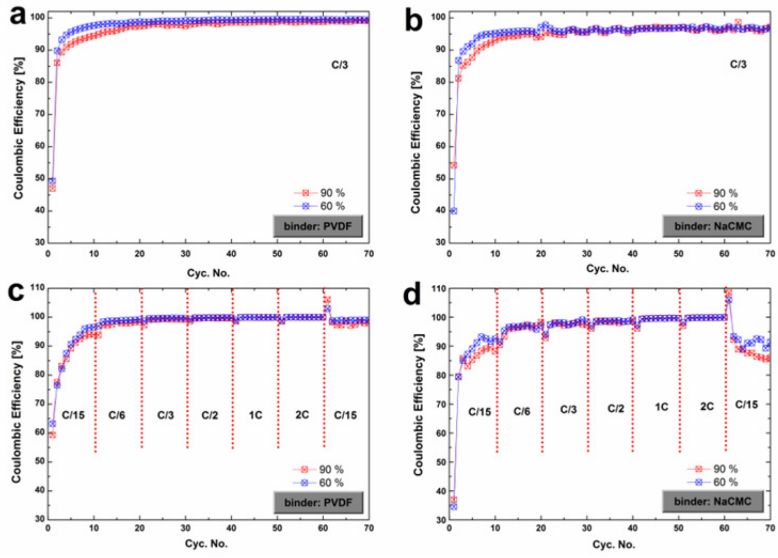

Figure A1 Coulombic Efficiencies of the SPCB based electrodes containing 90% and 60% of active materials in Li ion batteries: galvanostatic dis-/charge at C/3 for the (a), PVDF and (b), NaCMC based electrodes; and rate capability test for the electrodes using (c), PVDF and (d), NaCMC as the binder. (C = 300 mA g^{-1})

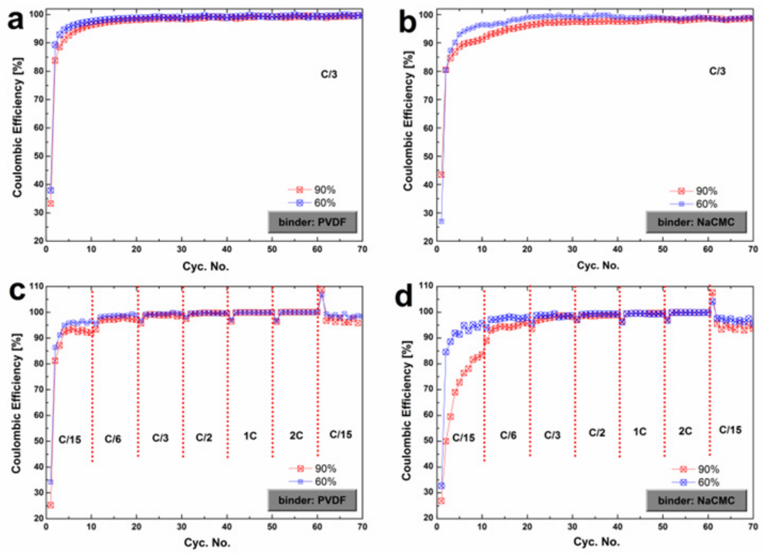

Figure A2 Coulombic Efficiencies of the SPCB based electrodes containing 90% and 60% of active materials in Na ion batteries: galvanostatic cycling at C/3 for the (a), PVDF and (b), NaCMC based electrodes; and rate capability test for the electrodes using (c), PVDF and (d), NaCMC as the binder. (C = 300 mA g^{-1})

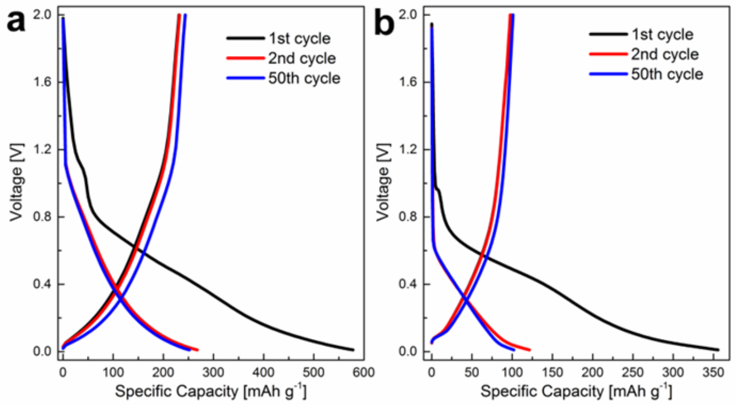

Figure A3 Voltage profiles of the SPCB based (a), Li and (b), Na ion anodes at 1st, 2nd and 50th cycle. Here the Li/Na ion battery anodes contain 60% SPCB and 40% NaCMC.

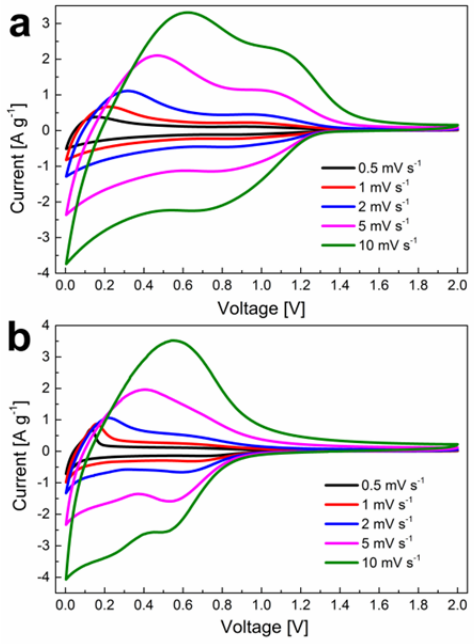

Figure A4 Cyclic voltammograms of the SPCB based (a), Li and (b), Na ion anodes at 1st, 2nd and 5th cycle. (scan rate: 0.5 mV s^{-1}) Here the Li/Na ion battery anodes contain 60% SPCB and 40% PVDF.